

Synthesis of high purity Au nanobelts via the one-dimensional self-assembly of triangular Au nanoplates

Jianhui Zhang, Huaiyong Liu, Zhenlin Wang, and Naiben Ming

Citation: [Applied Physics Letters](#) **91**, 133112 (2007); doi: 10.1063/1.2790578

View online: <http://dx.doi.org/10.1063/1.2790578>

View Table of Contents: <http://scitation.aip.org/content/aip/journal/apl/91/13?ver=pdfcov>

Published by the [AIP Publishing](#)

Articles you may be interested in

[Formation of one-dimensional self-assembled silicon nanoribbons on Au\(110\)-\(2×1\)](#)

Appl. Phys. Lett. **102**, 083107 (2013); 10.1063/1.4793536

[Optical rectification in self-assembled monolayers probed at surface plasmon resonance condition](#)

Appl. Phys. Lett. **95**, 021107 (2009); 10.1063/1.3179466

[Self-assembled monolayer cleaning methods: Towards fabrication of clean high-temperature superconductor nanostructures](#)

Appl. Phys. Lett. **86**, 154104 (2005); 10.1063/1.1899753

[Self-assembly of one-dimensional molecular and atomic chains using striped alkanethiol structures as templates](#)

Appl. Phys. Lett. **79**, 1685 (2001); 10.1063/1.1402648

[Guided self-assembly of Au nanocluster arrays electronically coupled to semiconductor device layers](#)

Appl. Phys. Lett. **77**, 373 (2000); 10.1063/1.126980

An advertisement for KeySight B2980A Series Picoammeters/Electrometers. The ad features a red and white color scheme. On the left, text reads 'Confidently measure down to 0.01 fA and up to 10 PΩ' and 'KeySight B2980A Series Picoammeters/Electrometers'. Below this is a red button with the text 'View video demo'. On the right, there is an image of the device and the KeySight Technologies logo.

Synthesis of high purity Au nanobelts via the one-dimensional self-assembly of triangular Au nanoplates

Jianhui Zhang,^{a)} Huaiyong Liu, Zhenlin Wang, and Naiben Ming

National Laboratory of Solid State Microstructures, Department of Physics, Nanjing University, Nanjing 210093, China

(Received 9 August 2007; accepted 7 September 2007; published online 27 September 2007)

High purity ($\sim 88\%$) gold nanobelts have been synthesized in the water/polyvinylpyrrolidone (PVP)/*n*-pentanol system created to realize the selective-adsorption of PVP on Au which directs Au to grow in belt form via the one-dimensional (1D) self-assembly of triangular Au nanoplates. These nanobelts present uniform thickness and lateral dimension, large aspect ratio up to 160, unique 60° angle end structure, and double-peak plasmon resonance property. The PVP directed 1D self-assembly method demonstrated here may provide a general route for the shape-selective synthesis of the other 1D functional nanostructures. © 2007 American Institute of Physics.

[DOI: 10.1063/1.2790578]

Nonspherical metal nanoparticles have been investigated widely in recent years because of their shape-dependent optical and electronic properties and applications in electronics, photonics, catalysis, biomedicine, and sensors.¹⁻¹⁷ As the most promising nanostructures, one-dimensional (1D) metallic nanoscale materials such as nanorods/nanowires/nanobelts of Cu, Ag, Au, Pd, Ni, Te, and Pb have become increasingly reported in the literature.^{2-4,7-15} However, the synthesis of Au nanobelts had remained a big challenge. Up to now, only Zhang *et al.* have synthesized high purity Au nanobelts (by a sonochemical route in the presence of glucose).¹² Recently, we have developed a simple versatile route based on the water/polyvinylpyrrolidone (PVP)/*n*-pentanol (WPN) system for the highly shape-selective synthesis of Ag, Au, and Pd triangular nanoplates,¹⁶ Au regular octahedra,¹⁷ and ZnO particles with lamellar or layer structures.^{16,18} Here, the unique WPN system has been extended to prepare the high purity Au nanobelts with large aspect ratio up to 160.

In a typical synthesis, 3.9 ml of distilled water was added into 60 ml of *n*-pentanol solution of PVP ($M_n=30\,000$, 1.5 g) in a conical flask with a ground stopper under stirring at room temperature. After 30 min, 1.5 ml of ethanol solution of $\text{HAuCl}_4 \cdot 4\text{H}_2\text{O}$ (0.024M) was added with stirring for 5 min. Then the mixture was heated at $95 \pm 1^\circ\text{C}$ in a constant temperature oven for one day. The obtained product was washed with ethanol three times by centrifugation and ultrasonication, and characterized by transmission electron microscopy (TEM), selected-area electron diffraction (SAED), scanning electron microscopy (SEM), and powder x-ray diffraction (XRD). Visible absorption spectra of the sample dispersed in ethanol were recorded on a U-3410 spectrophotometer. Infrared absorption spectra of the sample dispersed on the silicon substrate were collected using a far-field Fourier transform infrared spectrometer (Nicolet 5700).

As shown in Fig. 1(a), the product was dominated by the Au belts with lengths up to $20\ \mu\text{m}$. However, a lot of undesired particles such as large triangular and hexagonal plates

and small triangular plates and spheres were also observed. Furthermore, the belts could not be purified through centrifugation because the small particles usually attached to the lateral sides of the belts. Figure 1(b) shows a high-magnified SEM image of the belts. As seen in the figure, all belts were uniform in both lateral dimension ($\sim 130\ \text{nm}$) and thickness ($\sim 30\ \text{nm}$). Interestingly, the belts usually ended with the similar acute angle (60°) structure and edge length as the small triangular plates had. Obviously, our gold belts are different from the reported Au belts ending with a rectangled structure.¹²

Like the Au octahedra and triangular nanoplates in our previous reports,^{16,17} here the growth of the Au belts also involves the self-seeding process in which PVP acts as the main reductant. It has been found that the surface energies or crystallinity of the initial seeds are crucial for controlling the morphology of the final product.^{1-9,13,16-18} However, only changing the PVP amount can not achieve the uniform seeds for the growth of the high purity belts because the PVP reduction ability is relatively weak. To improve the belt purity, the uniform Au nanoparticles ($\sim 10\ \text{nm}$) were directly added to act as the seeds. In brief, 3 ml of aqueous $\text{HAuCl}_4 \cdot 4\text{H}_2\text{O}$ (0.03M) and 6 ml of aqueous sodium citrate (1.0%) were added sequentially into 360 ml of boiling water. After 15 min. of boiling, the objective Au nanoparticle suspension was obtained. A 3.9 ml of Au nanoparticle suspension was used instead of the distilled water in repeating the synthesis of the Au belts shown in Fig. 1 by using 4.5 g of PVP. As shown in Fig. 2(a), the Au belts with high purity up to 88% and average length up to $21\ \mu\text{m}$ were obtained. The formation of the undesired particles such as the small and large triangular plates was basically suppressed. As seen in

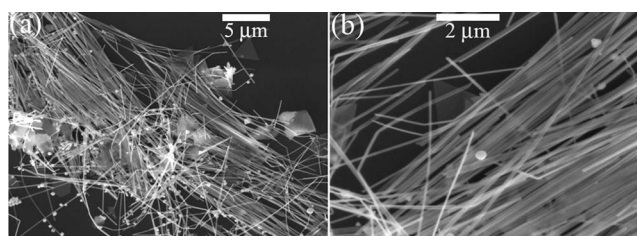


FIG. 1. Low (a) and high (b) magnified SEM images of Au nanobelts.

^{a)} Author to whom correspondence should be addressed. Electronic mail: zhangjh@nju.edu.cn

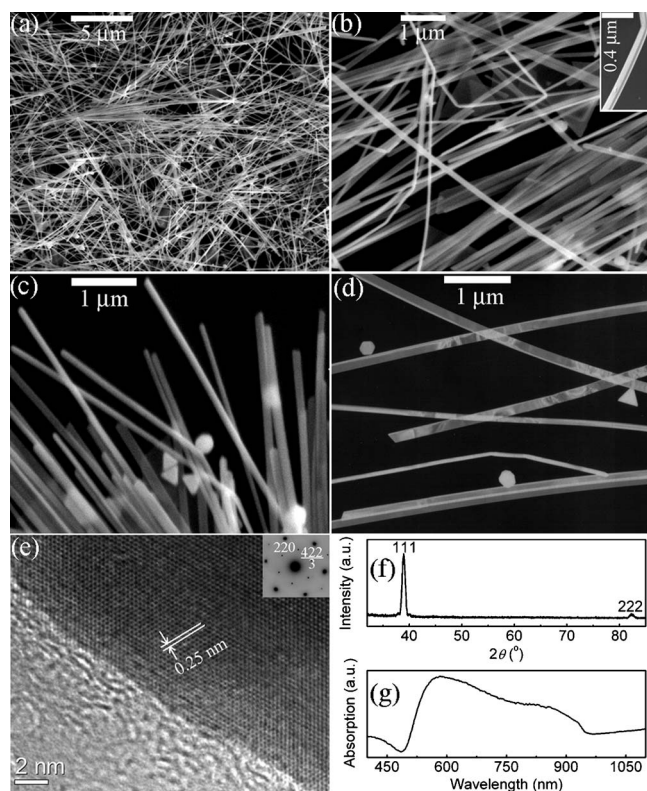


FIG. 2. Low (a) and high [(b)–(e)] magnified SEM or TEM images for the Au belts synthesized using Au nanoparticles. Insets of (b) and (e) show the corresponding high-magnified SEM image and SAED pattern. (f) and (g) show the XRD patterns and absorption spectrum of the Au belts, respectively.

the high-magnified SEM [Figs. 2(b) and 2(c)] and TEM [Fig. 2(d)] images, all the belts had uniform lateral dimension (~ 130 nm) and thickness (~ 40 nm) along their long belt axes. Like the belts shown in Fig. 1, all the Au belts also ended with the 60° angle structure which is identical to that of the byproduct—small triangular plates [see Figs. 2(c) and 2(d)]. To further characterize the crystallographic structure of the belts, the high-resolution TEM (HRTEM) images and the corresponding SAED patterns obtained from a belt lying flat on the support film with the electron beam perpendicular to the flat facets were recorded [see Fig. 2(e)]. The fringe spacing of 0.25 nm as well as the sixfold rotational symmetry displayed by the diffraction spots imply that all the lateral faces of the belts are presented by $\{111\}$ planes. The appearance of $(1/3)\{422\}$ reflection is consistent with the reported Ag belts⁹ but is contrary to the reported Au belts.¹²

XRD was used to assess the overall quality and purity of the Au belts. As seen in Fig. 2(f), only the (111) and (222) diffraction peaks were detected. This is a clear indication that the faces of these belts are primarily composed of $\{111\}$ planes, thus confirming the HRTEM results. The extinction spectra [Fig. 2(g)] of the Au belts dispersed in ethanol were also collected to evaluate the product quality and purity, because the optical properties of metal nanoparticles are highly dependent on the particle shapes.^{1–17} Like the reported Au belts,¹² our Au nanobelts also have two surface plasmon resonance (SPR) absorption peaks. One peak corresponding to the transverse short axes of the belts appears around 580 nm; the other peak around 862 nm can be attributed to the longitudinal SPR mode of the long axes of the belts. This

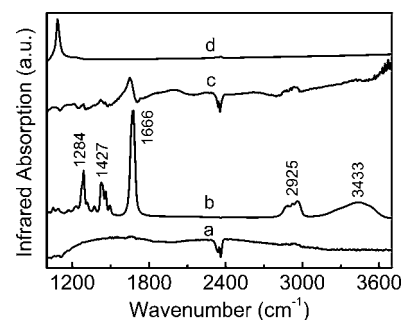


FIG. 3. Infrared absorption spectra of the silicon substrate (a), pure PVP (b), and the Au belts shown in Fig. 2 before (c) and after (d) 4 h of annealing at 900°C .

result and the XRD patterns actually reflect the high pure Au belts achieved by us.

Like the Au octahedra and nanosheets,^{1,13,16,17} here PVP may also direct the belt growth by selectively adsorbing onto the specific Au crystallographic planes. To confirm the scenario, the infrared absorption spectra were recorded for the Au belts shown in Fig. 2. For comparison, the spectra of pure PVP and the Au belts after 4 h of annealing at 900°C were also recorded. As shown in Fig. 3, PVP has some typical bond absorptions around 1284, 1427, 1666, 2925, and 3433 cm^{-1} arising from the absorptions of the $\text{N}\rightarrow\text{H}\rightarrow\text{O}$ complex, the pyrrolidone ring, and the bond vibrations of $\text{C}=\text{O}$, $\text{C}\text{--}\text{H}$, and $\text{O}\text{--}\text{H}$ of water impurity, respectively.¹⁹ The belts also show several typical PVP-related absorption bands that disappear after removing PVP by annealing, thus confirming the adsorption of PVP on the Au belts. Compared with pure PVP, in the Au belts, the band related to the $\text{C}\text{--}\text{H}$ bond vibration remains unvaried in position since the $\text{C}\text{--}\text{H}$ chain is inert to Au. However, the bands related to the $\text{N}\rightarrow\text{H}\rightarrow\text{O}$ complex, the pyrrolidone ring, and the bond vibrations of $\text{C}=\text{O}$ redshift to 1282, 1420, and 1639 cm^{-1} , respectively. These redshifts can be attributed to the bond weakening induced by the partial donation of O/N lone pair electrons of PVP to the vacant orbitals of the Au surface, namely, the coordination bond between the O/N atom of PVP and the specific Au crystallographic plane.

To monitor the Au belt growth process, the time-dependent TEM or SEM images for the products formed in the synthesis processes of the Au belts shown in Fig. 2 were recorded. After 4 h of reaction, the product was dominated by the mixture of small triangular plates and short belts with lengths of $<2\ \mu\text{m}$ and lateral dimension of ~ 130 nm. As seen in Fig. 4(a), all the belts ended with the 60° angle structure. The small triangular plates resembled the belt ends in the angle structure, edge length, and thickness, and usually tended to attach to the belt side faces with their edges. As the

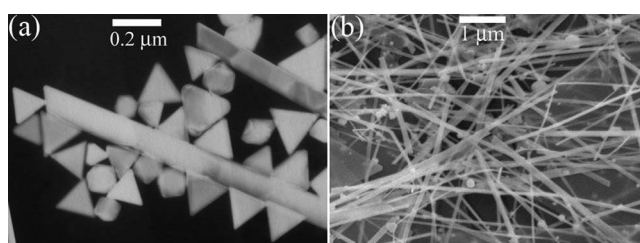
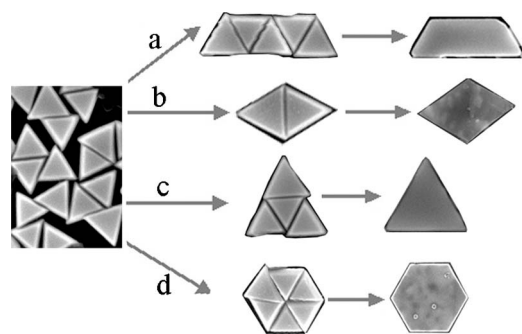


FIG. 4. Time-dependent TEM or SEM images of the products formed in the synthesis of the Au belts shown in Fig. 2 after reaction times of 4 h (a) and 8 h (b).



SCHEME 1. Observed assembly ways of the small triangular Au plates shown in Fig. 4(a) and the corresponding products.

reaction proceeded, the small triangular plates kept constant in edge length but decreased in yield ratio; meanwhile, the belts remained unvaried in lateral dimension, thickness, and acute angle structure but increased in length and yield ratio. After 8 h of reaction, the belts grew up to 2–10 μm in length [Fig. 4(b)]. After 24 h of reaction, the high purity belts with large aspect ratio of 160 were obtained (Fig. 2). These results indicate that the belts may grow by consuming the small triangular nanoplates.

Based on the above results, the following belt growth mechanism can be proposed. In our route, PVP prefers to adsorb onto the $\{111\}$ facets of the Au seeds by coordinating with Au with its O/N atoms. The following seed growth on the $\{110\}$ facets (without or with less PVP) leads to the formation of the triangular plates bounded by two triangular (111) basal facets and three $\{110\}$ side facets.^{13,16} Subsequently, due to the absence or insufficiency of the PVP capping,²⁰ the large van der Waals attractive forces²¹ between the $\{110\}$ side facets with high surface energy¹³ can induce the triangular plates to assemble along the $\langle 110 \rangle$ direction. In fact, we did find that the small triangular plates shown in Fig. 4(a) tended to self-organize with their $\{110\}$ side facets. As shown in Scheme 1(a), the triangular plates can assemble in 1D way and then recrystallize to form the single-crystal nanobelts with the same thickness and angle end structure as the triangular plates have. The interim products (in the 1D assembly process) such as the rhombic plates (originated from the paired-triangular plates) with discernible connection marks [see Scheme 1(b)] are luckily observed. The triangular plates can also assemble in two-dimensional (2D) way to form the large triangular [Scheme 1(c)] and hexagonal [Scheme 1(d)] plates. Obviously, 1D assembly is predominant in our route. This can be ascribed to the fact that 2D assembly may require higher monodispersity of the triangular plates in comparison to 1D assembly.

In summary, the Au nanobelts with high purity of up to ~88% have been synthesized via the PVP controlled 1D self-assembly of the triangular Au nanoplates. With unique 60° angle end structure, double-peak plasmon resonance property, uniform thickness and lateral dimension, and large aspect ratio of 160, the Au belts produced here may have broad potential applications in electronics, photonics, catalysis, biomedicine, and sensors. Furthermore, the PVP directed 1D self-assembly method demonstrated here may open up a general dimension for the highly shape-selective synthesis of the 1D functional nanostructures.

This work is supported by the NSFC (No. 10404013). The authors are grateful to P. Zhan and X.N. Zhao for their help on the SEM measurements.

- ¹F. Kim, S. Connor, H. Song, T. Kuykendall, and P. Yang, *Angew. Chem., Int. Ed.* **43**, 3673 (2004).
- ²G. Kawamura, Y. Yang, and M. Nogami, *Appl. Phys. Lett.* **90**, 261908 (2007).
- ³S. I. Shopova, C. W. Blackledge, A. T. Rosenberger, and N. F. Materer, *Appl. Phys. Lett.* **89**, 023120 (2006).
- ⁴J. Chen, B. J. Wiley, and Y. Xia, *Langmuir* **23**, 4120 (2007).
- ⁵J. E. Millstone, G. S. Métraux, and C. A. Mirkin, *Adv. Funct. Mater.* **16**, 1209 (2006).
- ⁶J. E. Millstone, S. Park, K. L. Shuford, L. Qin, G. C. Schatz, and C. A. Mirkin, *J. Am. Chem. Soc.* **127**, 5312 (2005).
- ⁷C. J. Murphy, T. K. Sau, A. M. Gole, C. J. Orendorff, J. Gao, L. Gou, S. E. Hunyadi, and T. Li, *J. Phys. Chem. B* **109**, 13857 (2005).
- ⁸C. J. Murphy, A. M. Gole, S. E. Hunyadi, and C. J. Orendorff, *Inorg. Chem.* **45**, 7544 (2006).
- ⁹Y. Sun, B. Mayers, and Y. Xia, *Nano Lett.* **3**, 675 (2003).
- ¹⁰Z. Liu, S. Li, Y. Yang, S. Peng, Z. Hu, and Y. Qian, *Adv. Mater. (Weinheim, Ger.)* **15**, 1946 (2003).
- ¹¹M. Mo, J. Zeng, X. Liu, W. Yu, S. Zhang, and Y. Qian, *Adv. Mater. (Weinheim, Ger.)* **14**, 1658 (2002).
- ¹²J. Zhang, J. Du, B. Han, Z. Liu, T. Jiang, and Z. Zhang, *Angew. Chem., Int. Ed.* **45**, 1116 (2006).
- ¹³C. Li, W. Cai, B. Cao, F. Sun, Y. Li, C. Kan, and L. Zhang, *Adv. Funct. Mater.* **16**, 83 (2006).
- ¹⁴A. Swami, A. Kumar, P. R. Selvakannan, S. Mandal, R. Pasricha, and M. Sastry, *Chem. Mater.* **15**, 17 (2003).
- ¹⁵T.-K. Huang, T.-H. Cheng, M.-Y. Yen, W.-H. Hsiao, L.-S. Wang, F.-R. Chen, J.-J. Kai, C.-Y. Lee, and H.-T. Chiu, *Langmuir* **23**, 5722 (2007).
- ¹⁶J. Zhang, H. Liu, Z. Wang, and N. Ming, *Adv. Funct. Mater.* **17**, 1558 (2007).
- ¹⁷J. Zhang, H. Liu, Z. Wang, and N. Ming, *Appl. Phys. Lett.* **90**, 163122 (2007).
- ¹⁸J. Zhang, H. Liu, Z. Wang, and N. Ming, *Appl. Phys. Lett.* **90**, 113117 (2007).
- ¹⁹Y. D. Cui, G. B. Yi, and L. W. Liao, *The Synthesis and Applications of Polyvinylpyrrolidone* (Science, Beijing, 2001), pp. 23–24.
- ²⁰The self-assembly of triangular plates can be suppressed by increasing the PVP capping via increasing the PVP amount. Typically, with increasing the PVP amount in the synthesis of the Au belts shown in Fig. 1 from 1.5 to 4.5 g, the main product changed from Au belts to small triangular Au particles [see Fig. 11(a) of Ref. 16].
- ²¹S. Biggs and P. Mulvaney, *J. Chem. Phys.* **100**, 8501 (1994).